RESEARCH ARTICLE | FEBRUARY 24 2015

Strangeness driven phase transitions in compressed baryonic matter and their relevance for neutron stars and core collapsing supernovae FREE

Ad. R. Raduta; F. Gulminelli; M. Oertel

AIP Conf. Proc. 1645, 86–91 (2015)
https://doi.org/10.1063/1.4909562

Strangeness driven phase transitions in compressed baryonic matter and their relevance for neutron stars and core collapsing supernovae

Ad. R. Raduta*, F. Gulminelli† and M. Oertel**

*IFIN-HH, Bucharest-Magurele, POB-MG6, Romania
†ENSICAEN, UMR6534, LPC ,F-14050 Caen cédex, France
**LUTH, CNRS, Observatoire de Paris, Université Paris Diderot, 5 place Jules Janssen, 92195 Meudon, France

Abstract. We discuss the thermodynamics of compressed baryonic matter with strangeness within non-relativistic mean-field models with effective interactions. The phase diagram of the full baryonic octet under strangeness equilibrium is built and discussed in connection with its relevance for core-collapse supernovae and neutron stars. A simplified framework corresponding to $(n,p,\Lambda)(+e)$-mixtures is employed in order to test the sensitivity of the existence of a phase transition on the (poorely constrained) interaction coupling constants and the compatibility between important hyperonic abundances and $2M_\odot$ neutron stars.

Keywords: neutron stars, core-collapse supernovae, phase transition, hyperons
PACS: 26.60.-c, 21.65.Mn, 64.10.+h

INTRODUCTION

Realistic description of a huge variety of astrophysical processes and structure of compact stars strongly rely on accurate microphysics input in terms of reaction rates and equation of state (EoS). In compact object physics a special attention is nowadays given to the properties of baryonic matter with densities above nuclear matter saturation density. The situation is challenging the more as not only nucleonic but also hyperonic degrees of freedom may be involved and the experimental data are too scarce to constrain the nucleon-hyperon (N-Y) and hyperon-hyperon (Y-Y) interactions over the relevant density domain. It was considered till recently that the EoS softening induced by the population of particle species other than nucleons makes strange baryonic content incompatible with the recently measured $2M_\odot$ PSR J1614-2230 [1] and PSR J0348+0432 [2] pulsars. This conclusion is now refuted based on various relativistic and non-relativistic models which show that hyperons may do exist in the core of massive stars provided that the $N-Y$ and $Y-Y$ interactions are sufficiently repulsive [3, 4, 5, 6, 7].

In the framework of a non-relativistic mean-field model with phenomenological interactions [8] it was recently shown that compressed baryonic matter with strangeness may face different types of first- and second-order phase transitions and that a strangeness-driven (SD) phase transition may be explored under strangeness equilibrium [9, 10]. Two phenomenological consequences have been worked out. It was shown that, in the vicinity of the critical points, the neutrino mean free path is severely reduced which is expected to impact on the star cooling [10]. Ref.[11] demonstrates within a spherical simulation that, if during the neutron star contraction after bounce the phase coexistence in reached, a mini-collapse is induced. All these studies have assumed that the hyperonic degrees of freedom may be generically described by the Λ-hyperon and the same interaction has been used.

The questions now rising are: a) what does the phase diagram plotted in Ref. [10] become if not only Λ but the whole baryonic octet is accounted for? and b) to what extent model and interaction dependent is the strangeness-driven phase transition of compressed baryonic matter? In the present contribution, we shall try to answer these issues. For the sake of straightforward comparison with thermodynamics of simple $(n,p,\Lambda)(+e)$-mixture, the first issue will be approached within the same Balberg and Gal model [8] previously used. As before, the stiffest parameterization, BGI, leading to the highest neutron star mass, will be employed. The occurrence of a strangeness-driven phase transition will be investigated in connection with both $N-Y$ and $Y-Y$ interactions and the possibility to produce $2M_\odot$ neutron stars. To avoid proliferation of uncontrolled coupling constants we will exclusively consider the (n,p,Λ) systems. The predilection for Λ is twofold: it has the best constrained potential and, according to several models, is the most abundant hyperonic species.

Exotic Nuclei and Nuclear/Particle Astrophysics (V). From Nuclei to Stars
AIP Conf. Proc. 1645, 86-91 (2015); doi: 10.1063/1.4909562

THE MODEL

In non-relativistic mean-field models, the total energy density of homogeneous baryonic matter is given by the sum of mass and kinetic energy densities of different particle species and the potential energy density:

$$e_B(\{n_i\}) = \sum_{i=n,p,\Lambda,\vec{\Sigma},\vec{\Xi}} \left(n_i m_i c^2 + \frac{\hbar^2}{2m_i}\tau_i \right) + e_{pot}(\{n_i\}) = e_B(n_B, n_S, n_Q), \tag{1}$$

where $n_B = \sum_i n_i B_i$, $n_S = \sum_i n_i S_i$, $n_Q = \sum_i n_i Q_i$ represent the baryon, strangeness and charge number densities, respectively, corresponding to the three good quantum numbers assuming equilibrium with respect to strong interaction. The particle and kinetic energy densities are expressed in terms of Fermi-Dirac integrals,

$$n_i = \frac{1}{2\pi^2\hbar^3}\left(\frac{2m_i}{\beta}\right)^{\frac{3}{2}} F_{\frac{1}{2}}(\beta\tilde{\mu}_i);\ \tau_i = \frac{1}{2\pi^2\hbar^5}\left(\frac{2m_i}{\beta}\right)^{\frac{5}{2}} F_{\frac{3}{2}}(\beta\tilde{\mu}_i), \tag{2}$$

with $F_\nu(\eta) = \int_0^\infty dx \frac{x^\nu}{1+\exp(x-\eta)}$. $\beta = T^{-1}$, m_i and $\tilde{\mu}_i$ denote, respectively, the inverse temperature, the effective i-particle mass and the effective chemical potential of the i-species self-defined by the single-particle density. The effective chemical potentials are related to the chemical potentials $\mu_i = \frac{\partial e_B}{\partial n_i}$ via $\tilde{\mu}_i = \mu_i - U_i - m_i c^2$ where $U_i = \frac{\partial e_{pot}}{\partial n_i}|_{n_j, j\neq i}$ are the self-consistent mean field single-particle potentials.

The potential energy density should in principle account for all possible couplings between nucleons and hyperons. Experimental data allow to satisfactorily constrain the N-N interaction close to normal nuclear matter saturation density and isospin symmetry. For values far from $(\rho_0, \delta = 0)$ the interaction potential is subject to large uncertainties. The uncertainties are even more serious in what regards the N-Y and Y-Y channels. Indeed, the single hyperon exotic nuclei, for which several experimental data are available, only provide information on $\Lambda-$, $\Xi-$ and, less certain, $\Sigma-$ well depths in symmetric nuclear matter at saturation density. The presently accepted values are $U_\Lambda^{(N)} \approx -30$ MeV, $U_\Xi^{(N)} \approx -14$ MeV. Double-Λ hypernuclei, for which only few data exist, constrain the $\Lambda-\Lambda$ interaction at a density few times smaller than the normal nuclear saturation density. As such, the coupling constants are adjusted to reproduce standard values of these potentials $U_C^{(C')}(n_{C'}) = \partial e_{pot}(n_C, n_{C'})/\partial n_C|_{n_C=0}$ at some reference density, obtained within a (model dependent) analysis of the available experimental data.

In their pioneering work [8], Balberg and Gal write the potential energy density as a sum over all possible two-particle interactions, $i, j = n, p, \Lambda, \Sigma^-, \Sigma^0, \Sigma^+, \Xi^-, \Xi^0$,

$$e_{pot}^{(BG)}(\{n_i\}) = \sum_{i,j} e_{ij}^{(BG)}(n_i, n_j), \tag{3}$$

and assume for the sake of simplicity that all channels can be described by the same functional,

$$e_{ij}^{(BG)}(n_i, n_j) = \left(1 - \frac{\delta_{ij}}{2}\right)(a_{ij} n_i n_j + b_{ij} n_{i3} n_{j3} + c_{ij} \frac{n_i^{\gamma_{ij}+1} n_j + n_j^{\gamma_{ij}+1} n_i}{n_i + n_j}), \tag{4}$$

where a_{ij}, c_{ij} and b_{ij} respectively stand for the long-range attraction, short-range repulsion and isovector interactions.

The expressions of single-particle potentials of the baryon C in pure C- and, respectively, C'-matter

$$U_C^{(C)}(n_C) = a_{CC} n_C + \frac{\gamma+1}{2} c_{CC} n_C^\gamma; \quad U_C^{(C')}(n_{C'}) = a_{CC'} n_{C'} + c_{CC'} n_{C'}^\gamma\ . \tag{5}$$

show that the particular form of Eq. (4), via the fixed potential, introduces a (probably artificial) correlation between the parameters governing repulsion and those governing attraction. We stress that the same holds for the microscopically based parameterization of Ref. [12], as we shall see in the following.

As explained at length in Refs. [9, 10] phase transitions are expected to occur in all systems subject to competing attractive and repulsive forces. The second law of thermodynamics implies that, in order for a system to be stable, the surface of energetic (entropic) potentials should be convex (concave). The negation of this statement shows that thermodynamical instabilities and convexity anomalies of the thermodynamic potentials imply one another.

Taking on board the full baryonic octet, the thermodynamics of pure baryonic matter and charge neutral baryonic+leptonic matter, as the one which constitutes stellar matter, was investigated in the three-dimensional space

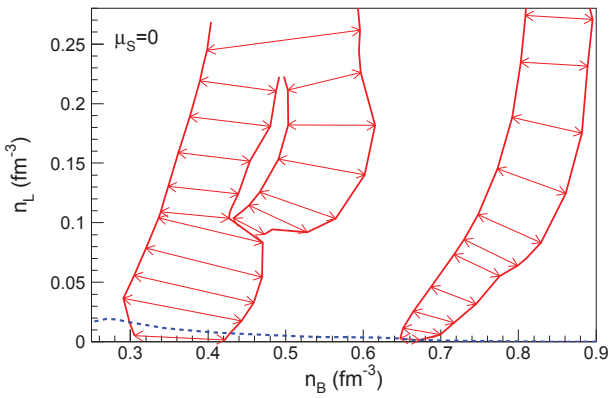

FIGURE 1. Phase diagram of the (n,p,Y,e)-system under strangeness equilibrium at T=1 MeV as provided by BGI parameterization [8] in the n_B-n_L-plane. The dotted curve marks the path corresponding to β-equilibrium. Figure taken from Ref. [14].

defined by baryonic, strangeness and charge (lepton) densities. The dimensionality of the order parameter, given by the eigen-vector associated to the negative eigen-values of the curvature matrix, was found, whenever a phase separation instability occurred, equal to one. Phase coexistence domains have been obtained as the locus of equal-(P,μ_B) points along constant-μ_S and constant-μ_L trajectories. We remind that the technique of Legendre transformation with respect to ($\mathscr{N}$-1) chemical potentials, where $\mathscr{N}$ is the number of components, is a standard procedure [13] meant to reduce the $\mathscr{N}$-dimensional Gibbs construction to one-dimensional Maxwell constructions.

The phase diagram of the $(n,p,\Lambda,\Sigma,\Xi)+e$ system at $\mu_S=0$ and T=1 MeV is plotted in Fig. 1 as a function of baryonic and leptonic densities. The thick lines mark the borders of the phase coexistence domains. The arrows mark the direction of the order parameter. As one may notice, up to three phase coexistence regions exist and a wide density domain corresponds to phase coexistence. The order parameter has important components along baryonic and strangeness densities and a modest component along the leptonic density. We stress that the persistence of the SD phase transition under the strongly non-compressible electron gas is due to the weak coupling between strangeness and leptonic densities and is at variance with what happens with the low density liquid-gas phase transition. The dotted line illustrates the β-equilibrium trajectory and shows that coexistence of phases with different strangeness enrichment may be explored also by neutron stars.

MODEL AND PARAMETER DEPENDENCE

In order to study which properties of the interaction potential are responsible for the occurrence of the SD phase transition, we shall turn to the simple case of a $(n,p,\Lambda)(+e)$-mixture which nevertheless accounts for all relevant degrees of freedom, B, Q, L, and consider the $N-Y$ and $Y-Y$ channels one at a time.

As the $Y-Y$ interaction is poorly known let us first consider that it does not exist and tune only the $N-Y$ interaction. The parameters $(\gamma,a_{\Lambda N})$ are considered as free and allowed to vary over wide domains of values. The third parameter, $c_{\Lambda N}$, is calculated out of the fixed value of the Λ-potential well depth in uniform saturated nuclear matter, $U_\Lambda^{(N)}$, here taken equal to -26 MeV, in agreement with the predictions of BGI. The left panel of Fig. 2 shows the $(\gamma,a_{\Lambda N})$ domain where a SD phase transition occur in symmetric (N,Λ) systems. It is a compact and wide domain; it is characterized by a strong long-range attraction. The behavior of $U_\Lambda^{(N)}$ as a function of non-strange baryonic density is spotted in the right panel of the same figure for several representative parameter sets sitting inside and outside the phase coexistence region and corresponding to various stiffnesses. For each case, the parameter values are mentioned on the figure. Because of the assumed form of the interaction potential, BG functionals correlate strong attraction in the low density range with strong repulsion in the high density range. For the considered parameter sets, a huge variety of behaviors is to be noticed.

The new precise measurements of neutron star masses close to $2M_\odot$ represent a validity test for any astrophysical equation of state. Though, as the recent literature testifies, this astronomical observation neither confirm nor rule out

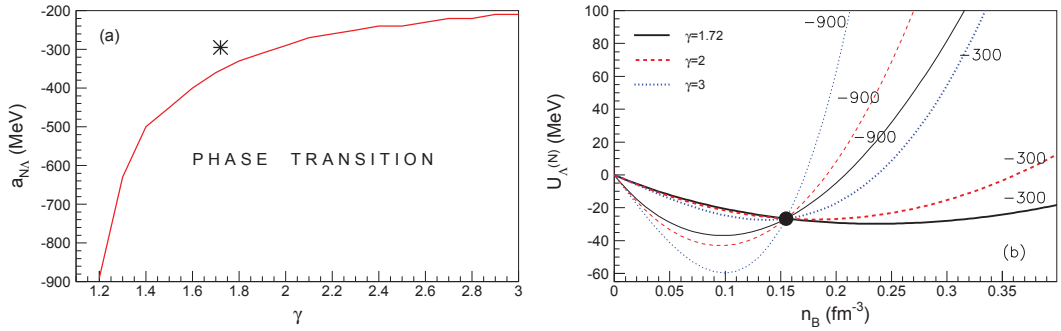

FIGURE 2. BG parameterization without Λ-Λ-interaction: (a) Limiting values of the coupling constant $a_{N\Lambda}$ for which, at different γ, the symmetric (N,Λ)-system at T=0 manifests strangeness driven phase transition along $\mu_S = 0$. The star marks the $(\gamma, a_{N\Lambda})$ values corresponding to the BSL $N-Y$-interaction (see text). (b) Nucleonic density dependence of the Λ potential in uniform symmetric nuclear matter $U_\Lambda^{(N)}(n_p+n_n)$ for different (γ,a_{YN}[MeV fm^3]) sets: (1.72,-900), (1.72,-300), (2,-900), (2,-300), (3,-900) and (3,-300). c_{YN} is determined such as $U_\Lambda^{(N)}(n_0)$=-26.6 MeV [8], see text. Figure taken from Ref. [14].

the presence of hyperons in neutron stars. The predictions of β-equilibrium EoS at T=0 for NS masses as a function of central density obtained by solving the TOV equations for hydrostatic equilibrium of a spherical non-rotating star are presented in the left panel of Fig. 3 for the same parameter sets as before. As highlighted by previous works, there exists a correlation among strong repulsion at high densities and maximum mass obtained for a NS. Out of the six considered $N-Y$ potentials, four lead to maximum masses largely exceeding the $2M_\odot$ limit. This result has nevertheless to be taken with caution because of the artificial absence of other hyperons than Λs. The inclusion of the full baryonic octet will obviously affect the relation between NS mass and radius and diminish the maximum NS mass.

The right panel plots the Λ relative abundance as a function of scaled distance from the star core for the maximum mass configuration and the same $N-Y$ interactions. With the exception of the strongest considered potential, (3, -900), which completely suppresses Λs, in all other cases important hyperonic abundances are obtained over sizable volume fractions. A direct comparison between the stiffness degree and the Λ fraction is, though, not possible because for each potential the maximum mass configuration corresponds to a different central density.

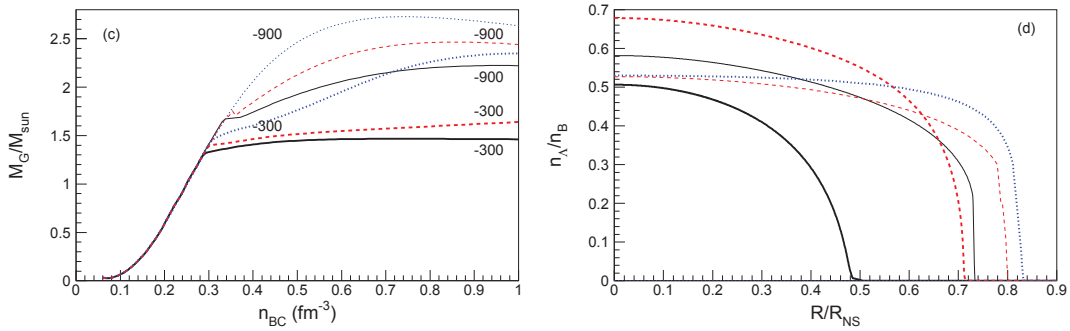

FIGURE 3. BG parameterization without Λ-Λ-interaction: (c) Neutron star mass as a function of central baryon density for the (γ,a_{YN}) sets considered in (b); (d) Λ relative abundances as a function of normalized distance from the star center for the maximum mass configuration and the (γ,a_{YN}) sets considered in (b). Figure taken from Ref. [14].

Over the last 15 years several Bruckner Hartree Fock calculations based on different bare $N-N$ and $N-Y$ interactions have been performed for both hypernuclei [15] and hypernuclear matter [12, 16] and various energy density functionals have been proposed. The parametrizations designed for hypernuclei are in general valid only at densities lower than normal nuclear matter density and, thus, inappropriate for star matter calculations. Two

parametrizations are conceived for hyper-nuclear matter. They rely on the same energy density functional,

$$e_{N\Lambda}^{(BSL)} = \left(a_\Lambda^0 + a_\Lambda^1 x + a_\Lambda^2 x^2\right) n_N n_\Lambda + \left(b_\Lambda^0 + b_\Lambda^1 x + b_\Lambda^2 x^2\right) n_N^{c_\Lambda} n_\Lambda + a_{\Lambda\Lambda}^{(BSL)} n_N^{c_{\Lambda\Lambda}^{(BSL)}} n_\Lambda^{d_{\Lambda\Lambda}+1}, \tag{6}$$

and differ in the coupling constant values as BHF calculations correspond to various treatments of the three body forces and YN potentials and predict significantly different Λ and Σ abundances. Because of its stiff $U_\Lambda^{(N)}$ behavior, in the following we shall discuss only the BSL case of Ref. [12].

Despite the functional dissimilarity between eqs. (4) and (6), the two parametrizations can be bridged via the Λ-potential in uniform symmetric matter,

$$U_\Lambda^{(N)}(n_N) = \left(a_\Lambda^0 + \frac{a_\Lambda^1}{2} + \frac{a_\Lambda^2}{4}\right) n_N + \left(b_\Lambda^0 + \frac{b_\Lambda^1}{2} + \frac{b_\Lambda^2}{4}\right) n_N^{c_\Lambda}, \tag{7}$$

which, in both cases, is a polynomial form of the baryonic density. Even more, eq. (7) can be mapped onto $\partial e_{pot}^{(BG)}/\partial n_\Lambda|_{n_\Lambda=0}$ provided that $\gamma = c_\Lambda = 1.72, a_{N\Lambda} = a_\Lambda^0 + a_\Lambda^1/2 + a_\Lambda^2/4 = -294.75$MeV fm^3, $c_{N\Lambda} = (b_\Lambda^0 + b_\Lambda^1/2 + b_\Lambda^2/4) = 462.75$ MeV fm$^{3\gamma}$. This means that, similarly to BG-functionals, also here long range attraction and short-range repulsion are correlated. The (1.72,-294.75) point is represented in Fig. 2 (a) by a star and sits outside the phase coexistence domain of a symmetric (N,Λ) mixture at strangeness equilibrium. We note that these values are very close to ($\gamma = 1.72$, $a_{\Lambda N} = -300$ MeV fm^3) for which $U_\Lambda^{(N)}(n_N)$ is depicted in Fig. 2.

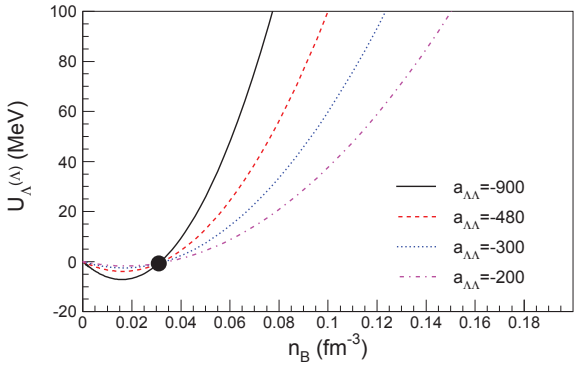

FIGURE 4. (Color online) Λ-potential in uniform Λ-matter as a function of density corresponding to BGI parameterization with modified Λ-Λ interaction: $a_{\Lambda\Lambda}$=-900, -480, -300 and -200 MeV fm^3 and $\gamma = 2$. Figure taken from Ref. [14].

We now turn to study the effect of $\Lambda\Lambda$ interaction on both phase transition and maximum NS mass. To keep the same framework as before, we shall stick to BGI parameterization in what regards the $N\Lambda$ channel and tune the $\Lambda\Lambda$ potential. As in the case of $N\Lambda$, the stiffness exponent γ and the parameter governing the low density attraction $a_{\Lambda\Lambda}$ are considered as free and let to cover domains defined by the values 1.2 and 3 and, respectively, -1000 and -100 MeV fm^3. The third parameter is deduced by the condition to have at $n_0/5$ a potential well depth in agreement with the experimental data, $c_{\Lambda\Lambda} = \left(U_\Lambda^{(\Lambda)}(n_0/5) - a_{\Lambda\Lambda} n_0/5\right) \cdot 2/(\gamma+1)/(n_0/5)^\gamma$. The adopted value shall be $U_\Lambda^{(\Lambda)}(n_0/5) =$ -0.67 MeV [17]. The results indicate that even a small $\Lambda\Lambda$ attraction added on the top of BGI $N\Lambda$ is sufficient to induce in symmetric (N,Λ) mixtures a phase transition.

Fig. 4 illustrates the strangeness density dependence of the $U_\Lambda^{(\Lambda)}$ in the particular case of $\gamma = 2$ and $a_{\Lambda\Lambda}$=-900, -480, -300, -200 MeV. As in the case of the N-Λ-channel, a strong attraction leads to a steep rise at high densities and a deep minimum localized at low densities, due to the fact that we fix the value at $n_0/5$ and the correlation between attraction and repulsion for the BG functional form.

Fig. 5 illustrates the predictions of these potentials in what concerns the NS gravitational mass as a function of central baryonic density (left panel) and Λ-relative abundance along the beta-equilibrium trajectory (right panel). The relative ordering of the different curves is easy to understand: the stronger is the $\Lambda\Lambda$ repulsion, the highest is the NS maximum mass and the lowest is the strangeness fraction. The small kink present on $M_G/M_\odot(n_{BC})$ curves around $1.5M_\odot$ stems from a narrow not Maxwell corrected phase coexistence region. All considered potentials largely fulfill

the criterion of producing NS mass larger than $2M_\odot$ and lead to non-negligible hyperonic abundances. Not only the repulsive behavior at high densities leaves a trace on the hyperonic content, but also the attractive one. Indeed, one can notice that an increased attraction is responsible for slightly shifting the strangeness production threshold to lower densities.

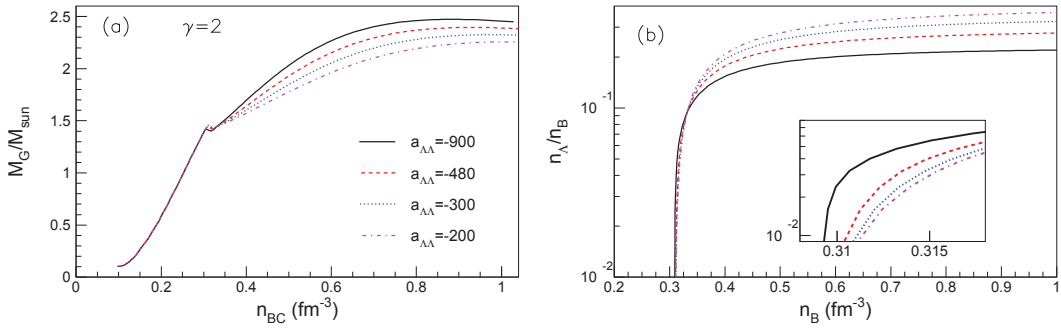

FIGURE 5. (a) Neutron star mass as a function of central density and (b) Relative Λ abundances as a function of baryonic density along the β-equilibrium path for the effective interaction potentials considered in Fig. 4. Figure taken from Ref. [14].

CONCLUSIONS

The phase diagram of charge neutral (baryonic+leptonic) matter, thought to constitute stellar matter, is spotted within a non-relativistic mean field model [8] with phenomenological effective interactions by accounting for the full baryonic octet. It is shown that, under strangeness equilibrium, a wide density domain corresponds to phase coexistence. The interplay between occurrence of phase transition, strengths of $N-Y$ and $Y-Y$ interactions and maximum NS mass is studied in the simplified case of a (n,p,Λ)-mixture by considering BG-type and microscopically motivated energy density functionals. Both $N-Y$ and $Y-Y$ interactions are seen to play a role in determining the existence of an instability. Within BG it comes out that an instability exists over a large parameter domain and the two solar mass limit is compatible with important hyperonic abundances. In contrast, BSL is stable with respect to phase separation. Nevertheless, phase separation can be induced by additionally accounting for $Y-Y$ interaction. We believe that there is no hyperon puzzle in the sense that important strangeness content can be accommodated within $2M_\odot$ NS. Though, a definite conclusion can be drawn only when more experimental constraints on the $N-Y$ and $Y-Y$ interactions will be available.

REFERENCES

1. P. Demorest *et al.*, Nature **467** 1081 (2010).
2. J. Antoniadis, P.C.C. Freire, N. Wex *et al.*, Science, 340, 6131 (2013).
3. I. Bednarek, P. Haensel, J.L. Zdunik, M. Bejger, and R. Manka, Astron. Astrophys. **543**, A157 (2012).
4. M. Oertel, A. F. Fantina, and J. Novak Phys. Rev. C **85**, 055806 (2012).
5. L. Bonanno and A. Sedrakian, Astron. Astrophys. **529**, A16 (2012).
6. S. Weissenborn, D. Chatterjee and J. Schaffner-Bielich,
7. S. Weissenborn, D. Chatterjee and J. Schaffner-Bielich, Phys. Rev. C **85**, 065802 (2012).
8. S. Balberg, and A. Gal, Nucl. Phys. **A625**, 435 (1997).
9. F. Gulminelli, Ad. R. Raduta, and M. Oertel Phys. Rev. C **86**, 025805 (2012).
10. F. Gulminelli, Ad. R. Raduta, M. Oertel, and J. Margueron, Phys. Rev. C **87**, 055809 (2013).
11. B. Peres, M. Oertel, J. Novak, Phys. Rev. D **87**, 043006 (2013).
12. G. F. Burgio, H.-J. Schulze, and A. Li, Phys. Rev. C **83**, 025804 (2011).
13. C. Ducoin, Ph. Chomaz, and F. Gulminelli, Nucl. Phys. **A771**, 68 (2006).
14. Ad. R. Raduta, F. Gulminelli, and M. Oertel, arXiv:1406.0395.
15. J. Cugnon, A. Lejeune, and H.-J. Schulze, Phys. Rev. C **62**, 064308 (2000); I. Vidana, A. Polls, A. Ramos, and H.-J. Schulze, Phys. Rev. C **64**, 044301 (2001); X.-R. Zhou, H.-J. Schulze, H. Sagawa, C.-X. Wu, and E.-G. Zhao, Phys. Rev. C **76**, 034312 (2007); H.-J. Schulze, Nucl. Phys. **A835**, 19 (2010).
16. H.-J. Schulze and T. Rijken, Phys. Rev. C **84**, 035801 (2011).
17. S. Aoki *et al.*, Nucl. Phys. **A828**, 191 (2009); J. K. Ahn *et al.*, Phys. Rev. C **88**, 014003 (2013).